Elsevier Editorial System(tm) for Applied Catalysis B: Environmental

Manuscript Draft

Manuscript Number:

Title: Cu-doped ZnO as efficient photocatalyst for the oxidation of arsenite to arsenate under visible light

Article Type: Research Paper

Keywords: photocatalysis; visible light; Cu-doped ZnO; arsenic; drinking water.

Corresponding Author: Dr. Giuseppina Iervolino, Engeneering

Corresponding Author's Institution: University

First Author: Vincenzo Vaiano

Order of Authors: Vincenzo Vaiano; Giuseppina Iervolino, Engeneering; Luigi Rizzo

Dear Editor,

I kindly ask you to consider for possible publication in "**Applied Catalysis B: Environmental"**, our research paper entitled:

Cu-doped ZnO as efficient photocatalyst for the oxidation of arsenite to arsenate under visible light

I would ask to publish our work because, at our knowledge, the use of ZnO doped with metals in photocatalytic oxidation of As(III) in As(V) under visible light is still scarce. In particular, a simple method for the synthesis of Cu-doped ZnO was proposed, able to obtain a visible light active photocatalyst.

We believe that our work can be interesting for the scientific community because it underlines the complete oxidation of As(III) to As(V) within only 30 minutes irradiation time. Moreover the experimental results have highlighted the efficiency of this photocatalyst also with different initial concentrations of As(III) in solution and in presence of radical scavengers, generally present in drinking water.

The manuscript matches the aims and scope of the journal because it is original and novel in relation to some fields relevant for the journal.

Sincerely,

The corresponding author.
Giuseppina Iervolino, PhD
Department of Industrial Engineering
University of Salerno, Via Giovanni Paolo II 132, 84084 Fisciano (Sa), Italy
Phone (+39) 089 964006 Email: giiervolino@unisa.it

***List of Three (3) Potential Reviewers**

1. Olga Sacco, University of Salerno, e-mail: osacco@unisa.it
2. M.C. Hidalgo,University of Seviglia, e-mail: mchidalgo@icmse.csic.es
3. Gupta Vinod Kumar, University of Johannesburg; e-mail: vinodfcy@iitr.ac.in

Cu-doped ZnO as efficient photocatalyst for the oxidation of arsenite to arsenate under visible light

V. Vaiano[1], G. Iervolino [1*], L. Rizzo[2]

[1] Department of Industrial Engineering, University of Salerno, via Giovanni Paolo II, 132, 84084 Fisciano (SA) Italy

[2]Department of Civil Engineering, University of Salerno, via Giovanni Paolo II, 132, 84084 Fisciano (SA) Italy

*Corresponding author: Tel: + 39 089 964006; Fax: + 39 089 9694057

E-mail: giiervolino@unisa.it

Abstract

In this work, photocatalytic oxidation of As(III) to As(V) by ZnO photocatalyts doped with Cu was investigated under visible light . Photocatalysts were successfully prepared by precipitation method. The obtained samples were characterized by N_2 adsorption at −196 C, X-Ray florescence analysis, X-ray diffraction, Raman spectroscopy, scanning electron microscopy and UV–vis reflectance analysis. In particular, according to XRD analysis all samples showed an hexagonal wurtzite structure with average crystallite sizes approximately in the range 32-33 nm. The doping with Cu allowed to obtain a decrease of band gap energy from 3.2 eV, typical of pure ZnO, to 2.92 eV. Photocatalytic oxidation tests under visible light showed that undoped ZnO is not able to oxidize the As(III) present in solution, while the complete conversion of As(III) to As(V) was achieved in the presence of Cu doped ZnO photocatalyst. In particular, the best photocatalytic activity was observed with ZnO doped with 1.08 mol% of Cu (1.08Cu_ZnO), within 120 min of exposure to visible light irradiation. The same result was observed under solar simulated radiation. Photocatalytic tests were carried out also in the presence of a real drinking water. In this case, the 1.08Cu_ZnO photocatalyst has maintained its activity, ensuring the complete oxidation of the As(III) in As(V) in 120 minutes of exposure under both visible light (emitted by LEDs) and solar simulated radiation.

Keywords: photocatalysis, visible light, Cu-doped ZnO, arsenic, drinking water.

Introduction

Arsenic is a very common element which can be found in rocks, water, air, animals and plants [1]. The toxic and carcinogenic effects of this element are widely known,

making it a serious threat to the environment and to human health [2]. To minimize these health risks, the World Health Organization (WHO) set the limit of maximum arsenic concentration in drinking water as low as $10\ \mu g \cdot L^{-1}$ [3, 4]. The prevalent forms of inorganic arsenic present in drinking water are As(III) (arsenite), and As(V) (arsenate) [5]. In particular, As(III) generally predominates in groundwater and it is also much more toxic, soluble, and mobile than As (V) [6]. Several processes/technologies have been used for arsenic removal from water so far, such as precipitation, adsorption, ion exchange and membrane systems [7, 8]. The main problem related to these processes is that they are effective only on the removal of As(V). So, the use of a pre-oxidation step is necessary to oxidize As(III) to As(V) in order to achieve the total arsenic removal with a subsequent separation process [9]. The oxidation can be achieved by conventional oxidants such as ozone [10], hydrogen peroxide, manganese dioxide [11], potassium permanganate, chlorine and chlorine dioxide. However, to avoid the formation of dangerous oxidation by-products and the presence of residuals in the treated water, photocatalysis can be a valid alternative [12]. Recently, several studies have been performed on the application of photocatalysis for the removal of arsenic from drinking water mainly using photocatalysts based on TiO_2 active under UV light irradiation or other kind of semiconductors such as Fe_3O_4 [4]. For example, in our previous work, MoO_x/TiO_2 photocatalytst was formulated and investigated in the photocatalytic oxidation of As(III) to As(V) in water [13]. With this photocatalyst, the complete oxidation of As(III) to As(V) took place, whereas unmodified titania was not able to oxidize all As(III) present in solution. Another example of a photocatalytic process reported in the literature for the oxidation of As (III) in As (V) deals with TiO_2 and zero-valent iron and an Xe lamp as light source to simulate sunlight [14]. However,

photocatalytic performances were strongly affected by the pH of the solution, being optimal results observed under acidic pH (3). Therefore, taking into account that drinking water has an almost neutral pH, it is interesting to formulate photocatalysts active under visible light, which allows to obtain the total oxidation of As(III) in As(V) even under neutral pH conditions. A novel bifunctional CuO-Fe_3O_4 material has been recently applied for As(III) removal through photooxidation and adsorption [4]. Interestingly, CuO-Fe_3O_4 nanoparticles can promote the photo-oxidation of As(III) to As(V) through CuO and As(V) adsorption through both CuO and Fe_3O_4 . Although these photocatalytic experiments were carried out in the presence of visible light ($\lambda > 420$ nm), the light source used was a 300 W Xe lamp, so characterized by a high energy consumption. Recently, the scientific community has developed a strong interest in another semiconductor: ZnO [15-24]. This photocatalyst has attracted an increasing attention due to its unique characteristics such as direct and wide band gap in the near-UV spectral region, strong oxidation ability, good photocatalytic property, and a large free-exciton binding energy [19, 25]. Moreover, ZnO is relatively cheaper compared to TiO_2 whereby the uses of TiO_2 are uneconomic for large scale water treatment operations [26]. In particular, as the removal of arsenic from drinking water is of concern, the use of ZnO for photocatalytic oxidation of As (III) to As (V) has been reported in the literature [27-31] and ZnO synthesis method affects its performance in the removal of contaminants from the water. Nidia Rivera-Reyna et al., observed that, in presence of UV light, the complete ZnO photocatalytic oxidation of As(III) was achieved within 180 min of treatment at pH 8 [27]. In order to improve the photocatalytic performance of ZnO, as well as to make it active even under visible light irradiation to decrease treatment costs, different strategies were proposed in literature for ZnO doping. Among these, the introduction of different

types of metal dopant into ZnO semiconductor, such as anionic dopant, cationic dopant and rare earth dopant, that could counter the recombination problem by enhancing the charge separation between electrons and holes, has been reported [32]. Anionic-doped ZnO photocatalyst enhanced the photocatalytic performances compared to that of pure ZnO. In the case of N doped ZnO system, the visible light absorption ability was increased [32, 33]. Moreover, the structural, optical, chemical, electrical and magnetic properties of ZnO can be tuned by the addition of selected cationic dopant, such as Cu^{2+}, Ni^{2+}, Co^{2+} and Mn^{2+}. Cation-doped ZnO has a lower band gap energy value, compared to the undoped ZnO. When cationic dopants were introduced as impurities in the ZnO crystal lattice, extra energy levels are added to the new photocatalyst [32]. Cu-doped ZnO photocatalyst has been proposed for the reactive black 5 degradation in presence of sunlight [34]. However, the literature concerning the use of ZnO doped with metals in photocatalytic oxidation of As(III) in As(V) under visible light is still scarce. Accordingly, the aim of this work was to investigate the photocatalytic performances of Cu-doped ZnO in the oxidation of As(III) in As(V). In particular a simple method for the synthesis of Cu-doped ZnO was proposed, able to obtain a visible light activated photocatalyst. Moreover, unlike of other works available in the scientific literature, a low energy consumption light source (LEDs) was investigated for the photocatalytic activation. The photocatalytic activity of the Cu-doped ZnO prepared at different Cu content and compared with the photocatalytic properties of undoped ZnO was assessed. The photocatalytic tests were carried out in aqueous matrices (deionized water solutions and real drinking water) using different As(III) initial concentrations and at the spontaneous pH of the solution.

2. Experimental

2.1 Photocatalyst preparation

2.2.1 Undoped ZnO catalyst

Undoped ZnO photocatalyst was prepared by the precipitation method starting from 5 g of zinc acetate dehydrate $ZnC_4H_6O_4$ (Aldrich, 99%) dissolved in 50 ml of distilled water and then by the slow addition of an aqueous solution obtained dissolving 2 g of NaOH (Aldrich, 99%) in 25 ml of distilled water at room temperature. Afterward, the generated precipitate was centrifuged, washed and calcined at 600 ◦C for 2 hours.

2.2.2 Cu-doped ZnO

Copper acetate hydrate $Cu(CH_3COO)$ was used in the doping procedure. Different amounts of $Cu(CH_3COO)$ were dissolved into the solution of $ZnC_4H_6O_4$ before to induce the precipitation with NaOH. The obtained precipitate was centrifuged, washed and calcined at 600 ◦C for 2 hours. The Cu nominal loading is expressed as molar percentage and it was evaluated through Eq.1:

$$\%mol\ Cu = \frac{nCu}{nCu+nZn} \cdot 100 \qquad \text{Eq.(1)}$$

Where:

nCu is the number of moles of $Cu(CH_3COO)_2$ used in the synthesis;

nZn is the number of moles of $Zn(CH_3COO)_2 \cdot 2H_2O$ used in the synthesis;

All the synthesized photocatalysts were listed in Table 1.

Table 1

2.2 Photocatalysts characterization

The catalysts were characterized using different techniques. Specific surface areas (SSA) of the samples were evaluated through Brunauer-Emmett-Teller (BET) method by N_2 adsorption with a Costech Sorptometer 1042 after a pretreatment at 150 °C for 1 h in He flow (99.9990 %). Total Cu content of the samples was evaluated by X-ray fluorescence spectrometry (XRF) in a thermos Fischer ARL QUANT'X EDXRF spectrometer equipped with a rhodium standard tube as the source of radiation and with Si-Li drifted crystal detector. The Raman spectra of the samples were recorded with a Dispersive MicroRaman system (Invia, Renishaw), equipped with 514 nm diode-laser, in the range 100-2000 cm^{-1} Raman shift. The crystal phases of ZnO based photocatalysts were determined by XRD analysis carried out on Brucker D8 diffractometer and the crystallite sizes were calculated using the Scherrer equation. The morphology of the prepared samples was examined using a scanning electron microscope (Assing, mod. LEO 420).

2.3 Photocatalytic activity tests

A pyrex cylindrical batch reactor (ID = 2.5 cm; height=18 cm) equipped with an air distributor device (Q_{air} = 150 cm^3/min under standard temperature and pressure conditions) and filled in with 100 ml of solution was used to test photocatalytic activity. The photocatalyst dosage was 3 g/l. Continuous mixing of the solution in the reactor was assured by a magnetic stirrer. The light source was a visible-LEDs strip (nominal power: 10W; light intensity: 32 mW/cm^2) with wavelength emission in the range 400-600 nm (Figure S1). The LEDs strip was rolled up around the external surface of the reactor so that the light source uniformly irradiates the reaction volume [35]. The reactor was left in dark condition for 2 hours before to

switch on visible LEDs. Photocatalytic reaction was carried out under light irradiation up to 3 hours. In order to evaluate the photocatalytic activity of the all prepared samples, preliminary tests with aqueous solutions containing 10 mg/l of methylene blue have been performed. In these conditions, the photocatalyst with the best performances in terms of the dye degradation was selected. Subsequently, photocatalytic tests for the oxidation of As(III) in As(V) in presence of visible light irradiation were performed. The effect of different initial As(III) concentration (1.5, 2.5 and 5 mg/l) was evaluated. Treated water samples were collected at fixed time to measure As(III) and As(V) concentration. In order to evaluate the radical scavengers effects, photocatalytic tests were performed also with real drinking water purposely contaminated by As(III). In the latter case, in addition to the tests with visible LEDs, the efficiency of the optimized photocatalyst was evaluated under simulated solar light by two 8 W Krypton-Argon lamps (SUN-GLO 8 W T5) whose emission spectrum is depicted in Figure S2. The lamps are positioned at a distance of about 30 mm from the photoreactor surface in order to irradiate the solution volume as much uniformly as possible.

2.4 Analytical measurements

Liquid samples were taken from the reactor at different times and analyzed with a Thermo Fisher Evolution 201 UV–Vis spectrophotometer to determine the change in dyes concentration through the measurement of the absorbance at $\lambda = 663$. A spectrophotometric method based on the formation of molybdenum blue [13] was used for the analysis of As(V) concentration at λ = 880 nm. The total arsenic concentration in the solution was analyzed introducing a previous step of oxidation of the As(III) present or residual in aqueous samples, through the addition of $KMnO_4$

aqueous solution (0.01 M). In this way As(III) was totally oxidized to As(V) and then analyzed with the molybdenum blue method in both untreated and treated solutions [2]. The As(III) and As(V) concentrations were calculated using the following equations:

$As_{tot} = As_{oxidized} - As_{reduced}$;

$As(III) = As_{oxidized} - As_{untreated;}$

$As(V) = As_{untreated} - As_{reduced}$;

3. Results and Discussion

3.1 Catalyst characterization

3.1.1 XRD analysis

XRD pattern of undoped and doped ZnO with different Cu content in the range 20-80° and 30-34°, respectively, showed five main peaks at 31.90°, 34.58°, 36.43°, 47.08° and 56.72°, respectively indexed to the (1 0 0), (0 0 2), (1 0 1), (1 0 2) and (1 1 0) planes, typical of the hexagonal wurtzite crystal structure (Fiugre 1) [36].

Figure 1

In particular, all the prepared samples showed the presence of wurtzite structural phase and no trace of copper related phase (such as metallic copper or oxides copper) was detected for 0.54 mol % and 1.08 mol % Cu doped sample. However, as doping percentage of Cu was increased up to 1.62 mol %, very weak peaks corresponding to CuO appeared [37], but they were found to grow in intensity as Cu doping was further increased (2.15 and 4.21 mol %).

Comparing doped and undoped ZnO in the range 30-34 ° (Figure 2), a slight shift of XRD peaks towards higher angle was observed.

Figure 2

This phenomenon is attributed to the narrowing of ZnO crystal lattice due to the substitution of Zn^{2+} by smaller Cu^{2+}, which suggest Cu^{2+} can easily substitute into ZnO crystal lattice [38, 39], without modify the crystal structure of ZnO [37]. As matter of fact, due to ionic radius dimension of Cu^{2+} (0.73˚A), which is very close to that of Zn^{2+} (0.74˚A), Cu ions can easily penetrate into ZnO crystal lattice [37]. Moreover, the doping process induced a slight decrease of photocatalysts crystallite size (Table 1). The average crystallite size of the pure ZnO was 35 nm. As the Cu content was increased, the average crystalline size decreased to 32 nm. According to the literature, this slight decrease in the crystallites size could be due to foreign impurities of Cu^{2+} in the ZnO lattice, which decreases the nucleation and the subsequent ZnO growth rate [40].

Accordingly, at smaller Cu doping concentrations, its ions can very well substitute Zn ions, but as Cu concentration increases, CuO starts to form cluster as impurity phase.

3.1.2 Raman analysis

Raman spectra in the range of 200-700 cm^{-1} of doped catalysts and undoped ZnO are showed in Figure 3.

Figure 3

In this range, there are four main bands at 333, 399, 438 and 583 cm^{-1}, related to ZnO [41]. The strong and sharp band observed at 438 cm^{-1} corresponds to the non-polar optical phonons E_2 (high) mode of ZnO. The features located at 331 and 383 cm^{-1} correspond to the multi-phonon scattering process $E_2H–E_2L$ and A_1 (phonons of ZnO crystal, respectively) [42]. The signal located at 583 cm^{-1} could be attributed to the E1, longitudinal optical phonon (LO), feature, associated with the formation of defects such as oxygen vacancy [43]. According to the literature, as the Cu doping concentration was increased, intensities of spectra decreased and the A1 transverse optical phonon (TO) mode vanished [44].

3.1.3 BET surface area and XRF results

The specific surface area (SSA) of all samples measured using BET gradually increased as Cu content was increased up to 1.08 mol % of Cu (Table 1).

Table 1

However, a decrease of the SSA for samples with higher Cu doping (from 1.62 mol %), was observed. These results are in agreement with literature about Cu doped photocatalyst [45]. XRF results show that the real Cu content is consistent with the corresponding value of nominal metal content, supporting the conclusion that synthesis process was successful (Table 1).

3.1.4 SEM analysis

The surface morphology of the undoped ZnO and Cu doped ZnO photocatalyst has been analyzed by SEM and the obtained results are presented in Figure 4.

Figure 4

In particular, for the sake of brevity, only the results for the ZnO samples, 1.08Cu_ZnO and 4.21Cu_ZnO were plotted. Both undoped and Cu-doped ZnO samples are composed of a number of non-uniform macro aggregates. Therefore the doping process did not affect the overall morphology of the photocatalysts.

3.1.5. UV–Vis diffuse reflectance spectra (UV–Vis DRS)

Optical absorption properties of the catalysts were studied throughUV–Vis DRS in the range of 300–900 nm (Figure 5).

Figure 5

Undoped ZnO showed the typical reflectance spectrum with a peak at about 390 nm. This behavior is due to the electron transition from O 2p to Zn 3d, corresponding to the transition from the valence band to the conduction band, according to the energy band structure of ZnO [46]. The doping of ZnO with Cu leads to an improvement in the intensity of light absorption in the UV region, according to the literature [38]. It

294 is worth noting that Cu doping resulted in an improvement of light absorption in the
295 visible region, which could make the samples effective under solar light irradiation
296 [47, 48].
297
298
299 The data obtained from UV–vis reflectance spectra were used to evaluate the band-
300 gap energy of the photocatalysts (Figure 6) summarized in Table 1.
301
302 **Figure 6**
303
304 As the Cu amount was increased, a decrease of band-gap energy (from 3.18 for
305 undoped ZnO to 2.91 eV for 4.21Cu_ZnO) was measured. The observed decrease
306 was due to the electronic transition from donor levels formed with dopants to the
307 conduction band of the host photocatalysts [49].
308
309 *3.2 Photocatalytic activity tests*
310 *3.2.1 Influence of Cu content*
311 The photocatalytic activity of undoped ZnO and Cu-doped ZnO photocatalysts was
312 evaluated trough the degradation of methylene blue (MB) (initial concentration 10
313 mg/l) under visible light (catalyst dosage: 3 g/l).
314 As the dopant content was increased from 0.54 to 1.08 mol%, discoloration
315 efficiency of MB increased, but further increases of dopant level resulted in a
316 decreased MB degradation efficiency (Figure 7).
317
318 **Figure 7**
319

In particular, 1.08Cu_ZnO photocatalyst showed the highest photodegradation efficiency (52% of discoloration after 180 min of irradiation) compared to undoped ZnO and the other doped samples. As reported in literature, The improved photocatalytic performance is attributed to the synergic effect of Cu and ZnO, oxygen vacancy, decrease in size and suppressing the recombination rate of the electron-hole pairs [38]. However, according to the literature, the increase in Cu content beyond the optimal value led to a decrease in photocatalytic activity since the excess dopant content would acts as a recombination center of electron and hole pairs [50].

Once obtained the optimal content of doping in ZnO, the best photocatalyst (1.08Cu_ZnO) was used for the photocatalytic oxidation of As(III) to As(V).

3.2.2 Control tests on As(III) photocatalytic oxidation

In order to confirm the photocatalytic results obtained in the case of MB discoloration, control tests with only visible LEDs (photolysis test), undoped ZnO, 1.08Cu_ZnO and 1.62Cu_ZnO in presence of visible light, were carried out to evaluate the contribution of each process in the oxidation of As(III) (Figure 8a) in As(V) (Figure 8b) in liquid samples.

Figure 8

During photolysis test, both As(III) concentration decrease (initial concentration 5 mg/L) and As(V) increase were negligible. In presence of the tested photocatalysts, only the As(III) adsorption on the photocatalyst surface was observed during the dark phase, without As(V) formation. As LEDs were switched on, undoped ZnO was

slightly effective for As(III) oxidation, whereas the two Cu-doped ZnO photocatalysts exhibited a very high photocatalytic activity toward the transformation of As(III) into As(V), even confirmed by the parallel increase of As(V) concentration in aqueous solution (Figure 9b). In particular, at fixed irradiation time, the photocatalytic performances of 1.08Cu_ZnO were better than those achieved for 2.15Cu_ZnO sample. The better oxidation efficiency (almost complete removal of As(III) after 120 minutes of irradiation time) was achieved in the case of 1.08Cu_ZnO photocatalyst, confirming the results observed in the case of MB photodegradation tests (Figure 7).

Our results on the efficiency of Cu doped ZnO for the photocatalytic oxidation of As(III) are consistent with those documented in a previous work [27]. However, the results obtained here seem extremely interesting as they show that our photocatalyst is effective even under visible light and at spontaneous pH (close to neutral values typical of drinking water). Although photocatalytic oxidation experiments of As(III) using ZnO have been reported in the literature, the best results in terms of As(III) oxidation (94% after 360 minutes of visible irradiation time) were obtained at pH equal to 8 [27]. The oxidation of As(III) in As(V) under visible light was investigated using Pt/TiO_2 nanotube electrode [51]. In this case, a bias was applied, and As(III) oxidation rate increased as a positive bias in the range 0.0 - 2.0 V was applied. In particular, As(III) in the cathodic cell was completely oxidized into As(V) after 280 minutes of irradiation time and 2.0 V of positive bias potential [51].

3.2.3 Optimization of catalyst dosage for photocatalytic tests

The determination of the optimal catalyst dosage was made testing different dosage of 1.08Cu_ZnO photocatalyst, in the range 0.75-4.5 g/l (Figure 9).

Figure 9

As the amount of catalyst in the solution was increased, an almost linear increase of photocatalytic efficiency up to a dosage of 3 g/l was observed (70% of As(V) yield obtained after 180 minutes of visible light irradiation). According to a previous work, the photocatalytic reaction mechanism on the ZnO based photocatalysts is expected to mainly proceed by $HO^{\cdot}$ radicals and to a lesser extent by the contribution of holes [27, 52]. Therefore, it is possible to argue that the increase in the catalyst loading dose up to 3g/l provides more active sites on the 1.08Cu_ZnO surface, resulting in an increased amount of hydroxyl radicals. Beyond 3g/l catalyst dosage, the photocatalytic performances decreased (37 % of As(V) yield with a dosage equal to 4.5 g/l against 70 % As(V) yield achieved with 3 g/l catalyst loading). The worsening of photocatalytic activity may be explained considering that with an increase of catalyst dosage in the aqueous solution, the light penetration through the solution becomes difficult [13]. Therefore 3 g/l of photocatalyst loading was considered as the optimum dose and it was used to evaluate the influence of initial As(III) concentration in aqueous solution and the effect of a real water matrix.

3.2.4 Effect of the initial concentration of As (III) on the photocatalytic process

The effect of the initial concentration of As(III) on the photocatalytic oxidation of As(III) to As(V) using 1.08Cu_ZnO catalyst was investigated too (Figure 10).

Figure 10

In particular, Figure 10a shows the decrease of As(III) concentration during the dark phase and during the visible light irradiation time for the three initial As(III) concentrations investigated (1.22, 2.5 and 5 mg/l), the behavior of As(V) is showed in Figure 10b. The formulated photocatalyst is effective in all the initial As(III) concentrations investigated. However, the process was strongly affected by the amount of As(III) adsorbed in dark conditions, in agreement with previous study [27]. As matter of fact, the irradiation time necessary to achieve the complete As(III) removal increased with the increase of the initial As(III) concentration in solution and in particular, at lowest tested initial As(III) concentration (1.22 mg/l), the optimized 1.08Cu_ZnO photocatalyst is able to ensure the complete removal of As(III) after only 30 minutes of visible light irradiation.

3.2.5 Photocatalytic tests in drinking water

The effectiveness of the process was also evaluated in drinking water whose chemical-physical characteristics are shown in Table 2. The results in terms of As(III) decrease and As(V) production are reported in Figure 11.

Figure 11

It is well known that ionic species like bicarbonates and chlorides act as radical scavengers in photocatalytic processes [53, 54], so it is interesting to understand if their presence, even in low concentrations as in this case, involves a change in the efficiency of the process. In particular, the comparison in terms of As(III) oxidized and As(V) present in solution in the case of (i) distilled water under visible LEDs, (ii) drinking water under visible LEDs and (iii) drinking water under solar lamp, is

shown. The difference between the two matrices (distilled and drinking water) is evident during the dark adsorption phase, where a higher adsorption of As(III) on the catalyst surface in the case of the distilled water matrix was observed with respect to the As(III) adsorption in drinking water. However, in the presence of visible light, the efficiency of the photocatalyst is maintained also in drinking water. It is worthy to note that, in the latter case, after 180 minutes of both visible light irradiation and simulated solar light, the As(V) concentration is almost equal to the As(III) initial concentration evidencing that the 1.08Cu_ZnO photocatalyst is able to completely oxidize As (III) into As (V) that is released in solution without occupying the active sites, similarly to what observed using MoO_x/TiO_2 photocatalysts in the arsenite oxidation to arsenate under UV light [2, 13, 53].

4. Conclusions

The possibility to obtain an efficient oxidation of As (III) in As (V) has been demonstrated in this work by applying a photocatalytic process based on the use of Cu-doped ZnO photocatalysts active under visible light. The characterization of the photocatalysts showed that the crystal structure of all the samples is hexagonal wurtzite with average crystallite sizes approximately in the range 32-33 nm. Moreover the doping with Cu allowed to obtain a decrease of band gap energy from 3.2 eV, typical of pure ZnO, up to 2.92 eV. The best photocatalytic performances were obtained with the catalyst prepared with 1.08 mol% of Cu (1.08Cu_ZnO). In particular, a complete oxidation of As(III) (at 5 mg/l initial concentration) to As(V) has been achieved within 120 min under visible LEDs. Moreover the experimental results have highlighted the efficiency of this photocatalyst also with different initial concentrations of As (III) in solution. In particular, the total oxidation of As(III) was

obtained after only 30 minutes of irradiation time starting from an initial concentration of As(III) equal to 1.22 mg/l. It is worthy to mention that these results were obtained under the spontaneous pH of the solution (almost neutral pH), typical of drinking water. Finally, the synthesized photocatalyst has shown excellent performances even in the presence of solar simulated light and radicals scavengers, typically present in drinking water. In the latter case, after 180 minutes under both visible light and simulated solar light, As(V) concentration is almost equal to the As(III) initial concentration, evidencing that the 1.08Cu_ZnO photocatalyst is able to completely oxidize the As (III) into As (V) that is released in solution (and consequently it can be removed by a conventional adsorption process) without saturating photocatalyst active sites. This result will make photocatalyst life longer, which together with high process efficiency under neutral conditions, makes this process more attractive compared to other photocatalytic processes investigated so far.

References

[1] C.K. Jain, I. Ali, Water Research 34 (2000) 4304-4312.

[2] V. Vaiano, G. Iervolino, D. Sannino, L. Rizzo, G. Sarno, Chemical Engineering Research and Design 109 (2016) 190-199.

[3] R.R. Shrestha, M.P. Shrestha, N.P. Upadhyay, R. Pradhan, R. Khadka, A. Maskey, M. Maharjan, S. Tuladhar, B.M. Dahal, K. Shrestha, Journal of Environmental Science and Health - Part A Toxic/Hazardous Substances and Environmental Engineering 38 (2003) 185-200.

[4] T. Sun, Z. Zhao, Z. Liang, J. Liu, W. Shi, F. Cui, Journal of Colloid and Interface Science 495 (2017) 168-177.

[5] R.M. Dhoble, S. Lunge, A.G. Bhole, S. Rayalu, Water Research 45 (2011) 4769-4781.

[6] V.K. Sharma, M. Sohn, Environment International 35 (2009) 743-759.

[7] P. Bahmani, A. Maleki, H. Daraei, M. Khamforoush, R. Rezaee, F. Gharibi, A.G. Tkachev, A.E. Burakov, S. Agarwal, V.K. Gupta, Journal of Colloid and Interface Science 506 (2017) 564-571.

[8] M. Bhaumik, C. Noubactep, V.K. Gupta, R.I. McCrindle, A. Maity, Chemical Engineering Journal 271 (2015) 135-146.

[9] M. Bissen, F.H. Frimmel, Acta Hydrochimica et Hydrobiologica 31 (2003) 97-107.
[10] M.-J. Kim, J. Nriagu, Science of The Total Environment 247 (2000) 71-79.
[11] W. Driehaus, R. Seith, M. Jekel, Water Research 29 (1995) 297-305.
[12] A. Nikolaou, L. Rizzo, H. Selcuk, Control of disinfection by-products in drinking water systems, 2007.
[13] V. Vaiano, G. Iervolino, D. Sannino, L. Rizzo, G. Sarno, A. Farina, Applied Catalysis B: Environmental 160-161 (2014) 247-253.
[14] M.J. López-Muñoz, A. Arencibia, Y. Segura, J.M. Raez, Catalysis Today 280 (2017) 149-154.
[15] P. Goyal, S. Chakraborty, S.K. Misra, Environmental Nanotechnology, Monitoring and Management 10 (2018) 28-35.
[16] S. Duo, R. Zhong, Z. Liu, J. Wang, T. Liu, C. Huang, H. Wu, Journal of Physics and Chemistry of Solids 120 (2018) 20-33.
[17] P. Pascariu, I.V. Tudose, M. Suchea, E. Koudoumas, N. Fifere, A. Airinei, Applied Surface Science 448 (2018) 481-488.
[18] T. Iqbal, M.A. Khan, H. Mahmood, Materials Letters 224 (2018) 59-63.
[19] V. Vaiano, G. Iervolino, Journal of Colloid and Interface Science 518 (2018) 192-199.
[20] V. Vaiano, M. Matarangolo, J.J. Murcia, H. Rojas, J.A. Navío, M.C. Hidalgo, Applied Catalysis B: Environmental 225 (2018) 197-206.
[21] C. Jaramillo-Páez, J.A. Navío, M.C. Hidalgo, Journal of Photochemistry and Photobiology A: Chemistry 356 (2018) 112-122.
[22] R. Saravanan, S. Agarwal, V.K. Gupta, M.M. Khan, F. Gracia, E. Mosquera, V. Narayanan, A. Stephen, Journal of Photochemistry and Photobiology A: Chemistry 353 (2018) 499-506.
[23] L. Gnanasekaran, R. Hemamalini, R. Saravanan, K. Ravichandran, F. Gracia, S. Agarwal, V.K. Gupta, Journal of Photochemistry and Photobiology B: Biology 173 (2017) 43-49.
[24] M.H. Dehghani, P. Mahdavi, I. Tyagi, S. Agarwal, V.K. Gupta, Desalination and Water Treatment 57 (2016) 24359-24367.
[25] A. Janotti, C.G. Van de Walle, Rep. Prog. Phys. 72 (2009) 126501/126501-126501/126529.
[26] N. Daneshvar, D. Salari, A.R. Khataee, Journal of Photochemistry and Photobiology A: Chemistry 162 (2004) 317-322.
[27] N. Rivera-Reyna, L. Hinojosa-Reyes, J.L. Guzman-Mar, Y. Cai, K. O'Shea, A. Hernandez-Ramirez, Photochem. Photobiol. Sci. 12 (2013) 653-659.
[28] M. Arabnezhad, M. Shafiee Afarani, A. Jafari, International Journal of Environmental Science and Technology (2017).
[29] K. Khwamsawat, J. Mahujchariyawong, S. Danwittayakul, Using ZnO nanorods coated porous ceramic monolith to remove arsenic from groundwater, Key Engineering Materials, 2017, pp. 756-765.
[30] A.A. Alswata, M.B. Ahmad, N.M. Al-Hada, H.M. Kamari, M.Z.B. Hussein, N.A. Ibrahim, Results in Physics 7 (2017) 723-731.
[31] C. Miranda, P. Santander, J. Matschullat, B. Daus, J. Yáñez, H.D. Mansilla, Journal of Advanced Oxidation Technologies 19 (2016) 276-283.
[32] K.M. Lee, C.W. Lai, K.S. Ngai, J.C. Juan, Water Research 88 (2016) 428-448.
[33] M. Batzill, E.H. Morales, U. Diebold, Phys. Rev. Lett. 96 (2006) 026103/026101-026103/026104.

[34] T. Arai, S.-i. Senda, Y. Sato, H. Takahashi, K. Shinoda, B. Jeyadevan, K. Tohji, Chemistry of Materials 20 (2008) 1997-2000.
[35] G. Iervolino, V. Vaiano, D. Sannino, L. Rizzo, V. Palma, Applied Catalysis B: Environmental 207 (2017) 182-194.
[36] O. Yayapao, T. Thongtem, A. Phuruangrat, S. Thongtem, Materials Science in Semiconductor Processing 39 (2015) 786-792.
[37] S. Singhal, J. Kaur, T. Namgyal, R. Sharma, Physica B: Condensed Matter 407 (2012) 1223-1226.
[38] A.N. Kadam, T.G. Kim, D.S. Shin, K.M. Garadkar, J. Park, Journal of Alloys and Compounds 710 (2017) 102-113.
[39] S.P. Meshram, P.V. Adhyapak, D.P. Amalnerkar, I.S. Mulla, Ceramics International 42 (2016) 7482-7489.
[40] P.K. Sharma, M. Kumar, A.C. Pandey, Journal of Nanoparticle Research 13 (2011) 1629-1637.
[41] Q. Zhang, J.-K. Liu, J.-D. Wang, H.-X. Luo, Y. Lu, X.-H. Yang, Industrial & Engineering Chemistry Research 53 (2014) 13236-13246.
[42] Q.-P. Luo, X.-Y. Yu, B.-X. Lei, H.-Y. Chen, D.-B. Kuang, C.-Y. Su, The Journal of Physical Chemistry C 116 (2012) 8111-8117.
[43] V. Vaiano, M. Matarangolo, O. Sacco, D. Sannino, Applied Catalysis B: Environmental 209 (2017) 621-630.
[44] P. Ilanchezhiyan, G.M. Kumar, M. Subramanian, R. Jayavel, Materials Science and Engineering: B 175 (2010) 238-242.
[45] P. Pongwan, K. Wetchakun, S. Phanichphant, N. Wetchakun, Res. Chem. Intermed. 42 (2016) 2815-2830.
[46] L. Zhang, Y. Yang, R. Fan, J. Yu, L. Li, Journal of Materials Chemistry A 1 (2013) 12066-12073.
[47] S. Kuriakose, B. Satpati, S. Mohapatra, Physical Chemistry Chemical Physics 17 (2015) 25172-25181.
[48] P. Bandyopadhyay, A. Dey, R. Basu, S. Das, P. Nandy, Current Applied Physics 14 (2014) 1149-1155.
[49] W. Wang, M.O. Tadé, Z. Shao, Chemical Society Reviews 44 (2015) 5371-5408.
[50] P. Chen, Journal of Materials Science: Materials in Electronics 27 (2016) 2394-2403.
[51] Y. Qin, Y. Li, Z. Tian, Y. Wu, Y. Cui, Nanoscale Research Letters 11 (2016) 32.
[52] M.E. Pena, G.P. Korfiatis, M. Patel, L. Lippincott, X. Meng, Water Research 39 (2005) 2327-2337.
[53] G. Iervolino, V. Vaiano, L. Rizzo, G. Sarno, A. Farina, D. Sannino, Journal of Chemical Technology and Biotechnology 91 (2016) 88-95.
[54] A. Ziylan-Yavaş, N.H. Ince, Chemosphere 162 (2016) 324-332.

Table 1.

Photocatalyst	**Cu nominal amount [mol %]**	**Cu measured amount (XRF) [mol%]**	***SSA [m^2/g]**	**Band gap energy [eV]**	****Crystallite size [nm]**
ZnO	-	-	5.5	3.19	35
0.54Cu_ZnO	0.54	0.6	5.6	3.02	35
1.08Cu_ZnO	1.08	1.2	6.6	2.92	32
1.62Cu_ZnO	1.62	1.5	5.8	2.94	32
2.15Cu_ZnO	2.15	2.2	5.1	2.94	33
4.21Cu_ZnO	4.21	4.1	4.9	2.91	33

*B.E.T. method

**Scherrer equation

Table 2. Physical and chemical characteristics of drinking water

pH	7.2
Conductivity, µS/ cm	181
Total hardness,∘F	4.00
Sodium, mg /l	7.05
Potassium, mg /l	7.30
Calcium, mg /l	18.27
Magnesium, mg /l	5.99
Chlorides (Cl^-),mg /l	8.20
Sulfates (SO_4^{2-}),mg /l	2.90
Bicarbonates (HCO_3^-),mg /l	103.7
Nitrates (NO_3^-),mg /l	2.00

Figures

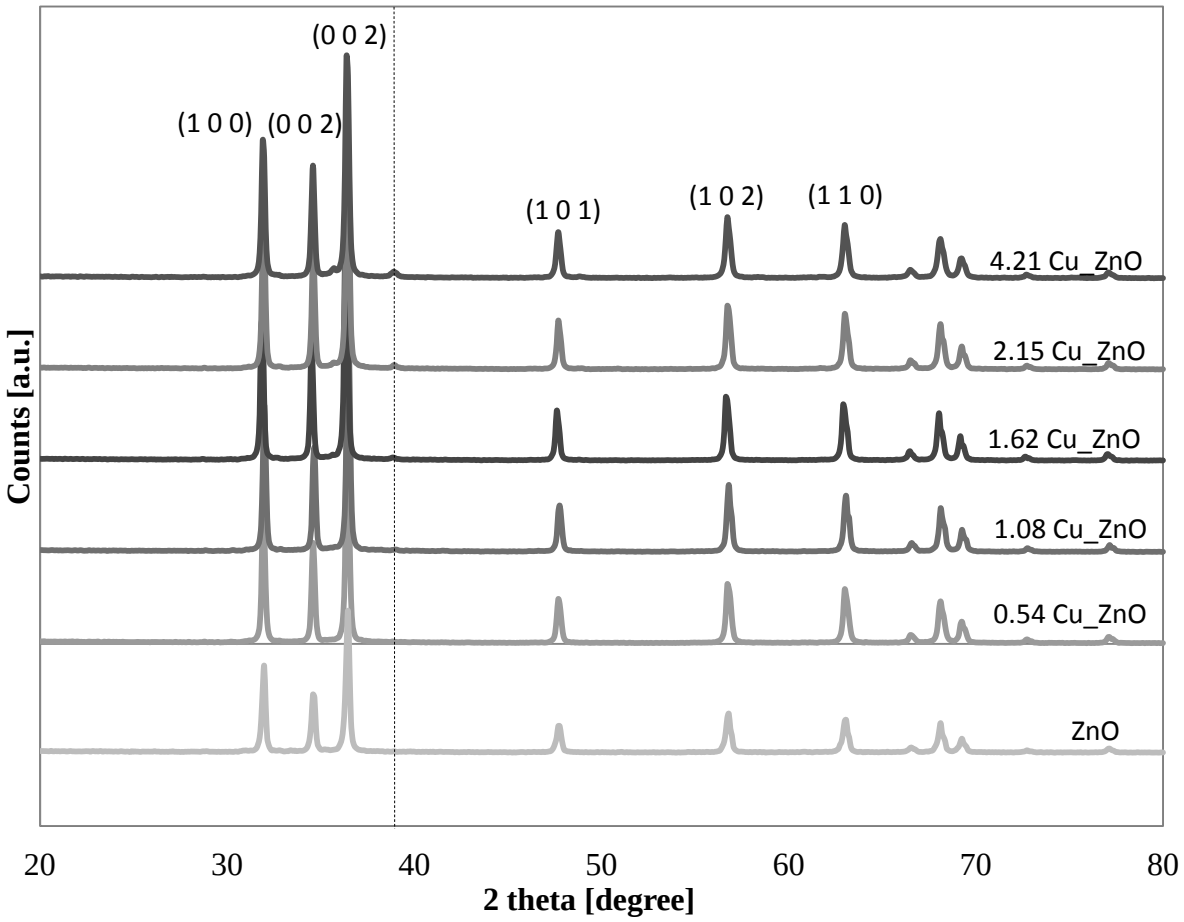

Figure 1: XRD spectra of undoped ZnO and Cu-doped ZnO photocatalysts in the range 20–80°

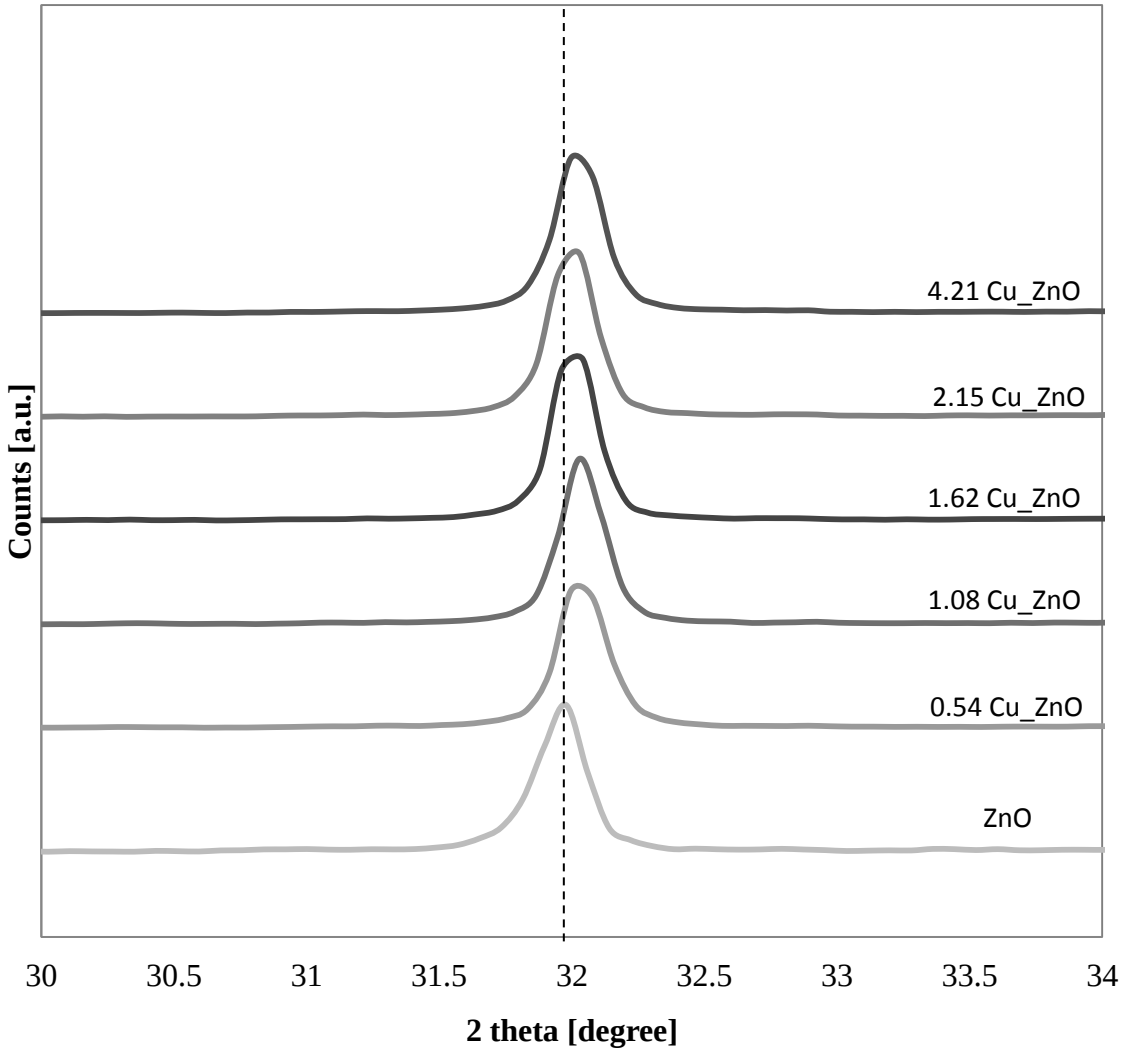

Figure 2: XRD patterns of undoped ZnO and Cu-doped ZnO photocatalysts in the range 30–34°

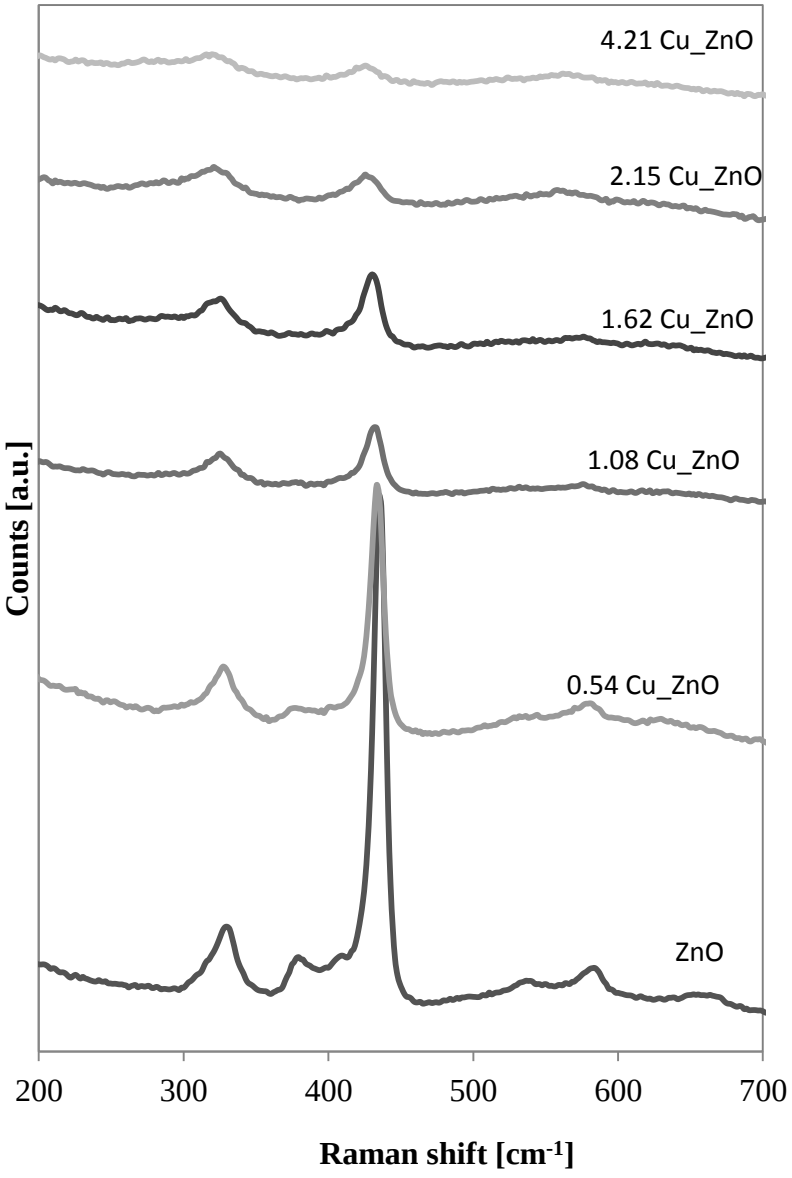

Figure 3: Raman spectra of undoped ZnO and Cu-doped ZnO photocatalysts in the range 200-700 cm^{-1}

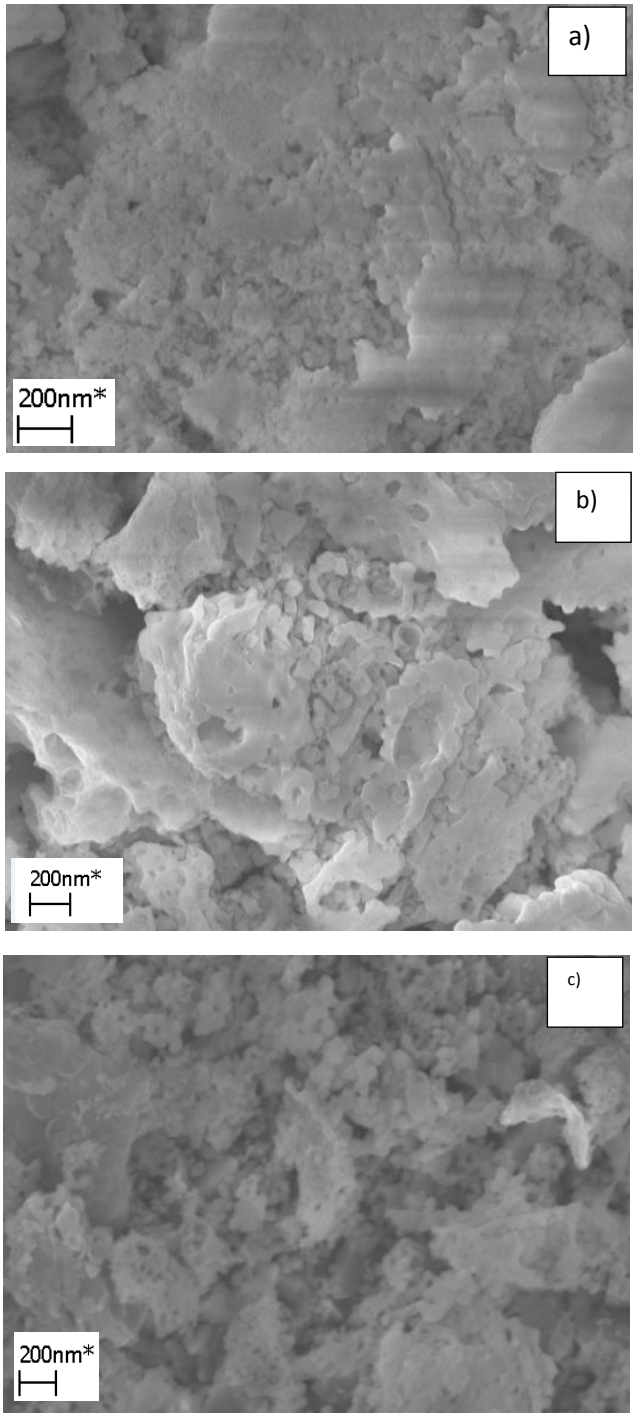

Figure 4: SEM images of undoped ZnO (a), 1.08Cu_ZnO (b) and 4.21Cu_ZnO (c) photocatalyst

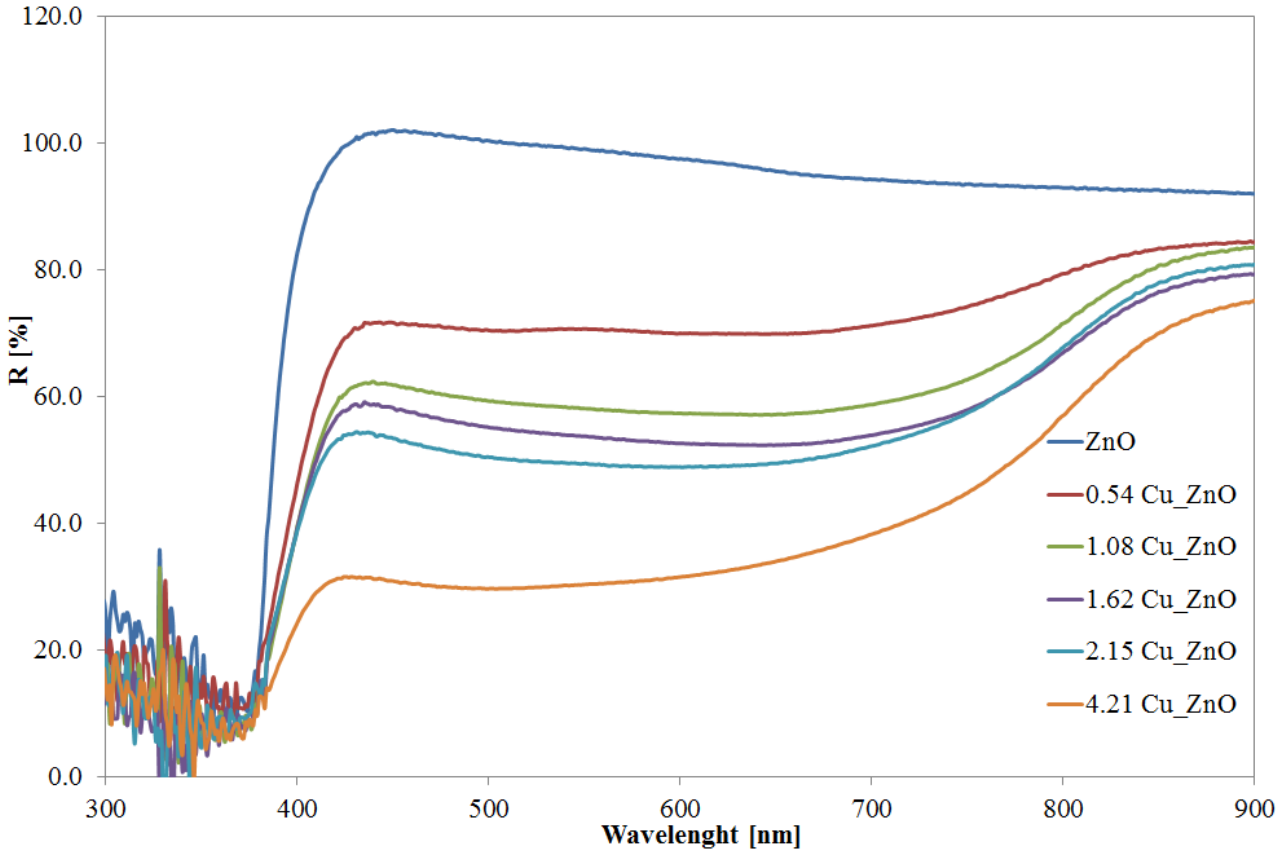

Figure 5: UV-visible reflectance spectra of ZnO and Cu-doped ZnO photocatalysts with different Cu contents.

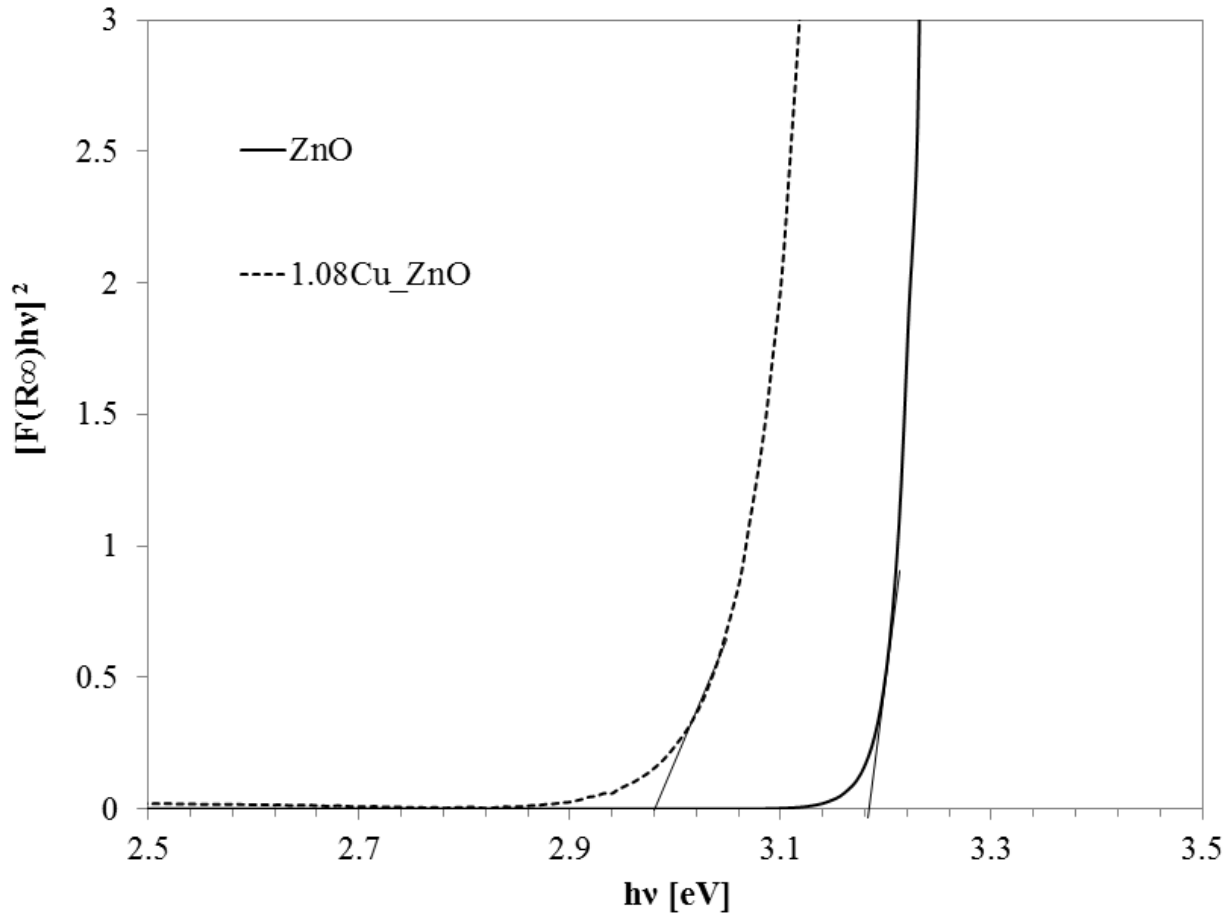

Figure 6: Evaluation of band gap for undoped ZnO and 1.08Cu_ZnO photocatalyst.

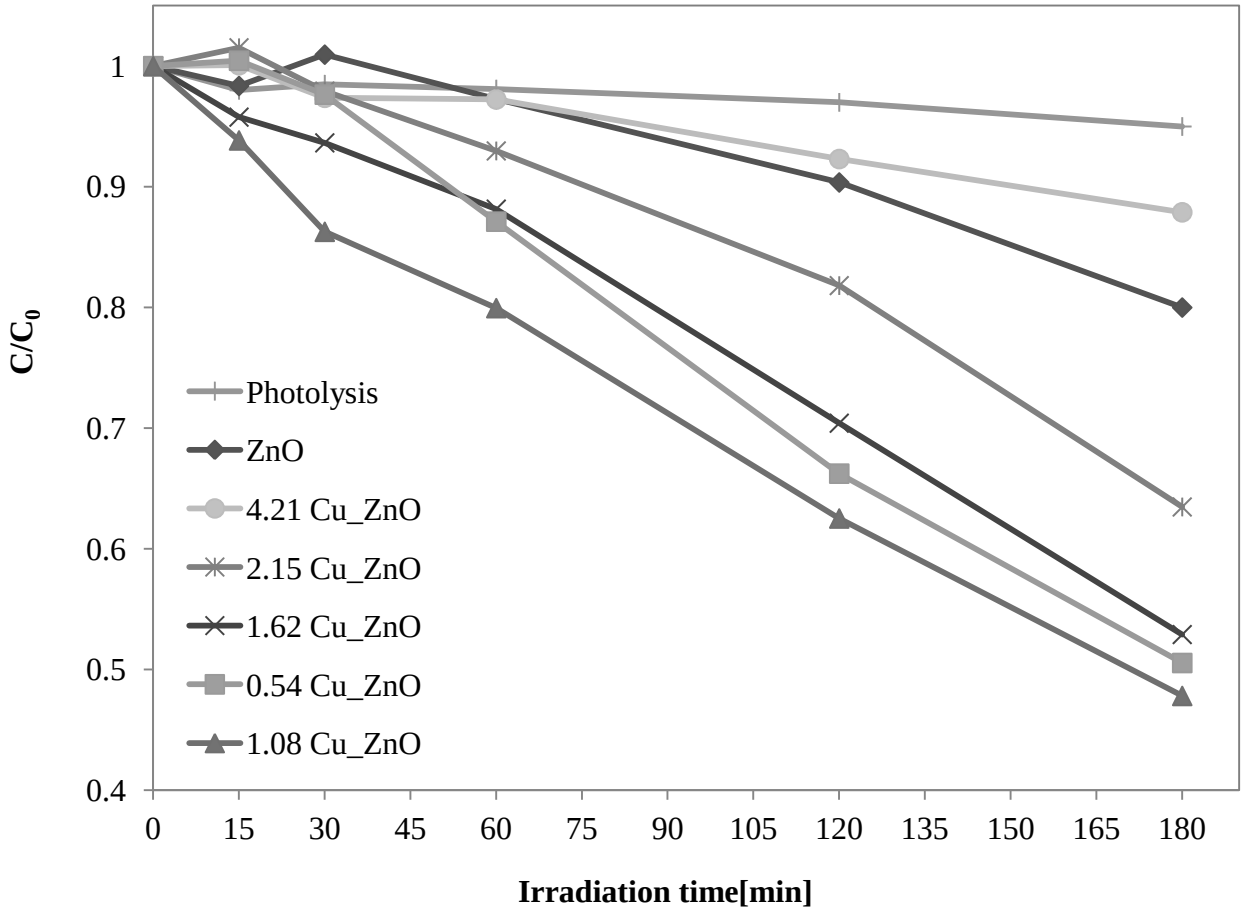

Figure 7: Behavior of methylene blue relative concentration during the irradiation time for all the photocatalysts; methylene blue initial concentration: 10 mg/l; catalyst dosage: 3 g/l.

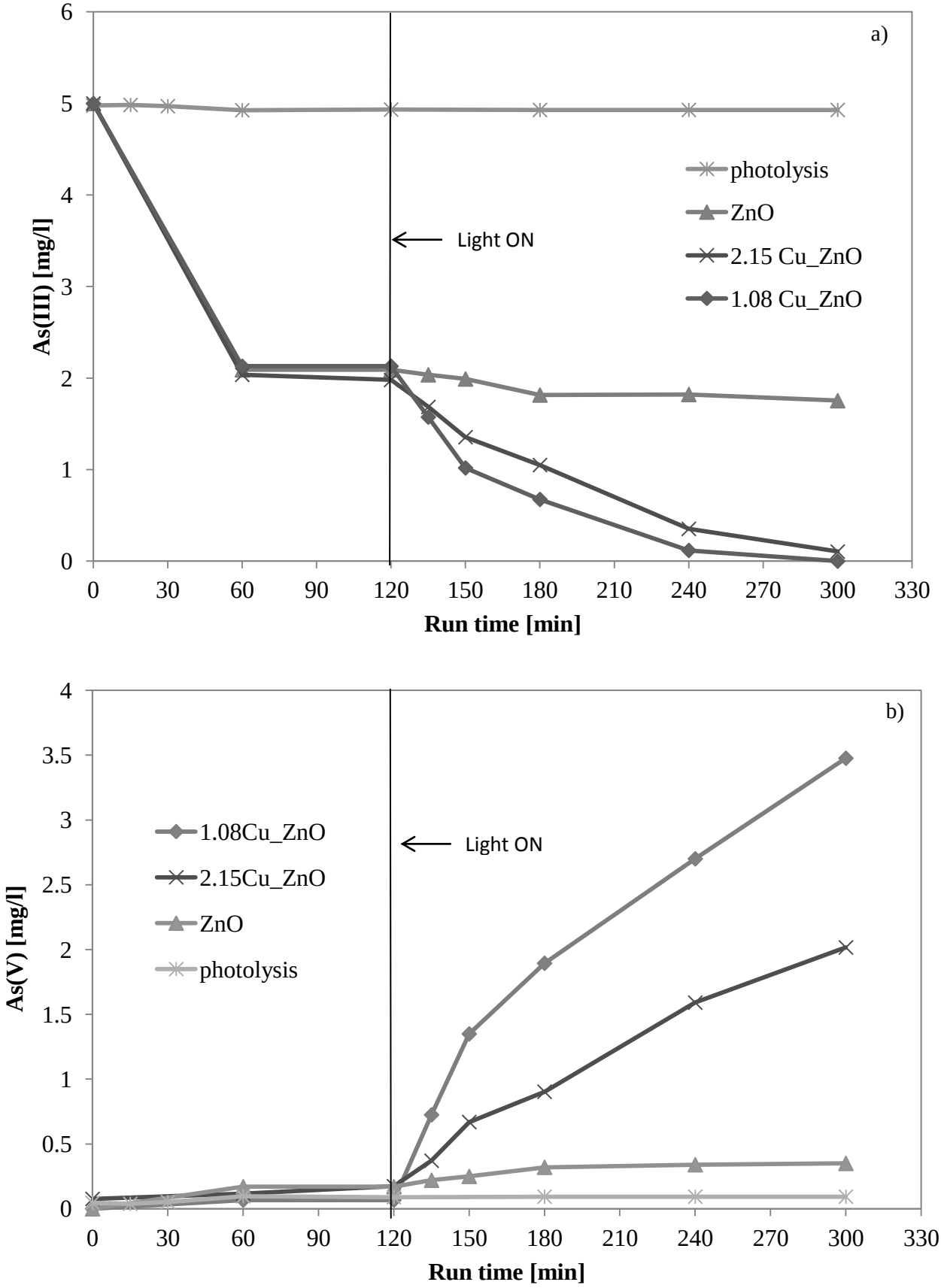

Figure 8: Control tests for the photocatalytic oxidation of As(III). Initial As(III) concentration: 5 mg/l. Catalyst dosage: 3 g/l. Behavior of As (III) (a) and As(V) (b) concentration.

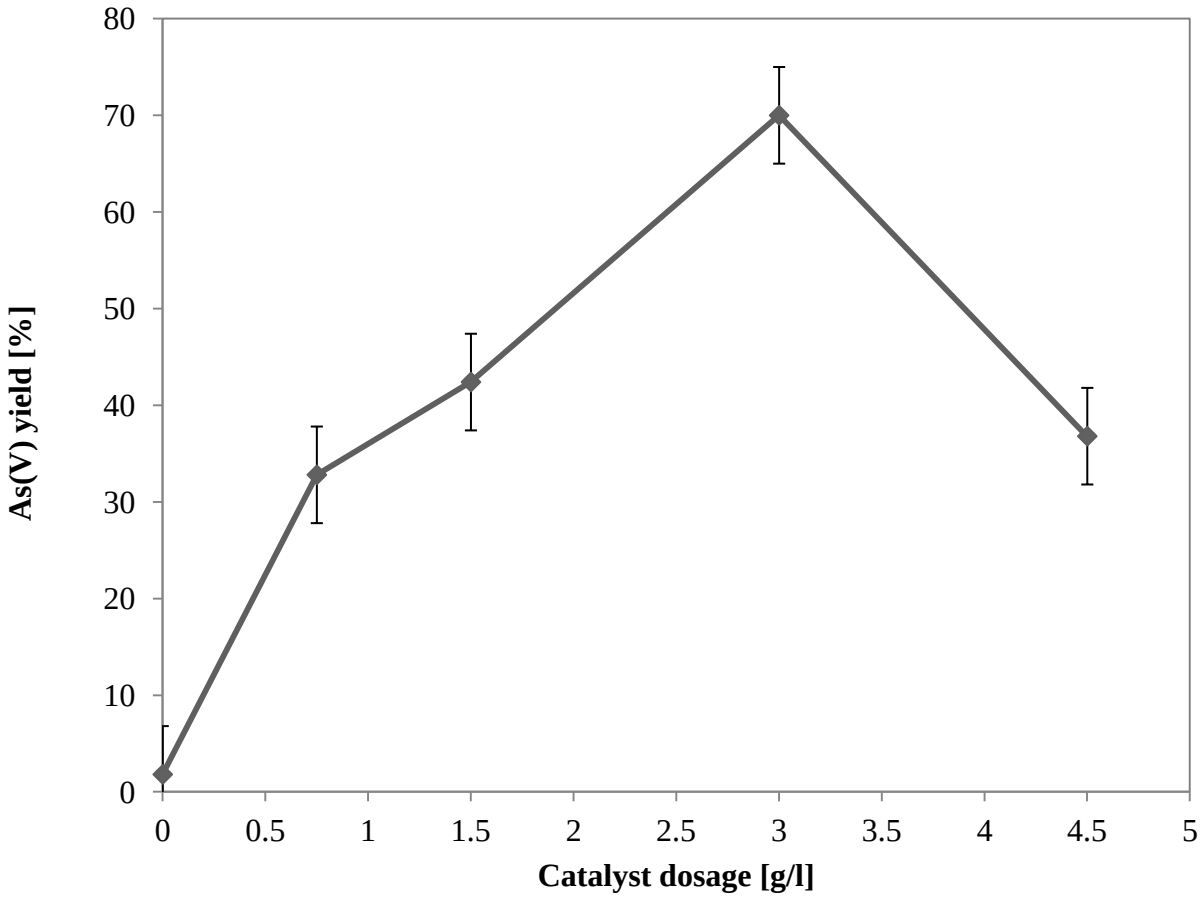

Figure 9: As(V) yield after 3 hours of irradiation time as a function of catalyst dosage. Initial As(III) concentration: 5 mg/l; photocatalyst: 1.08 Cu_ZnO

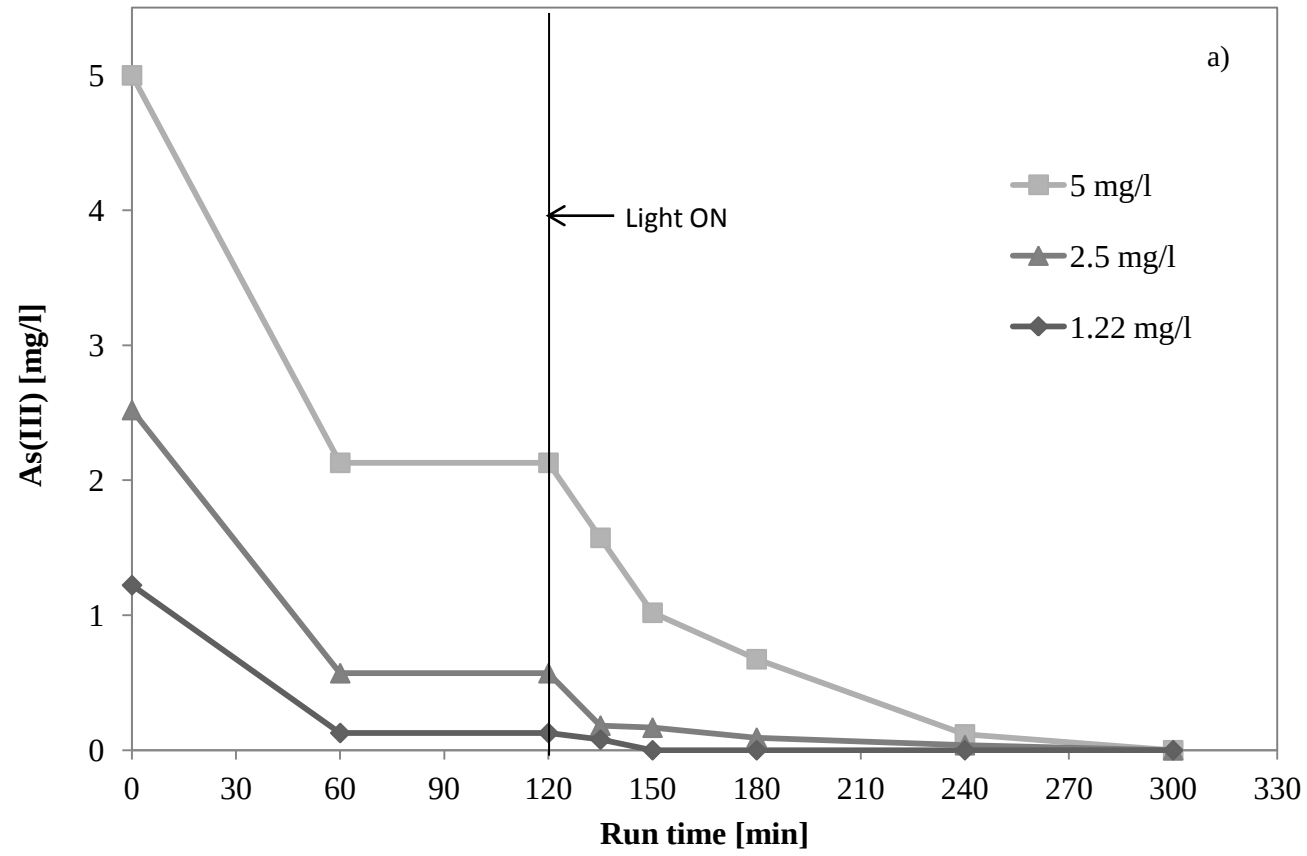

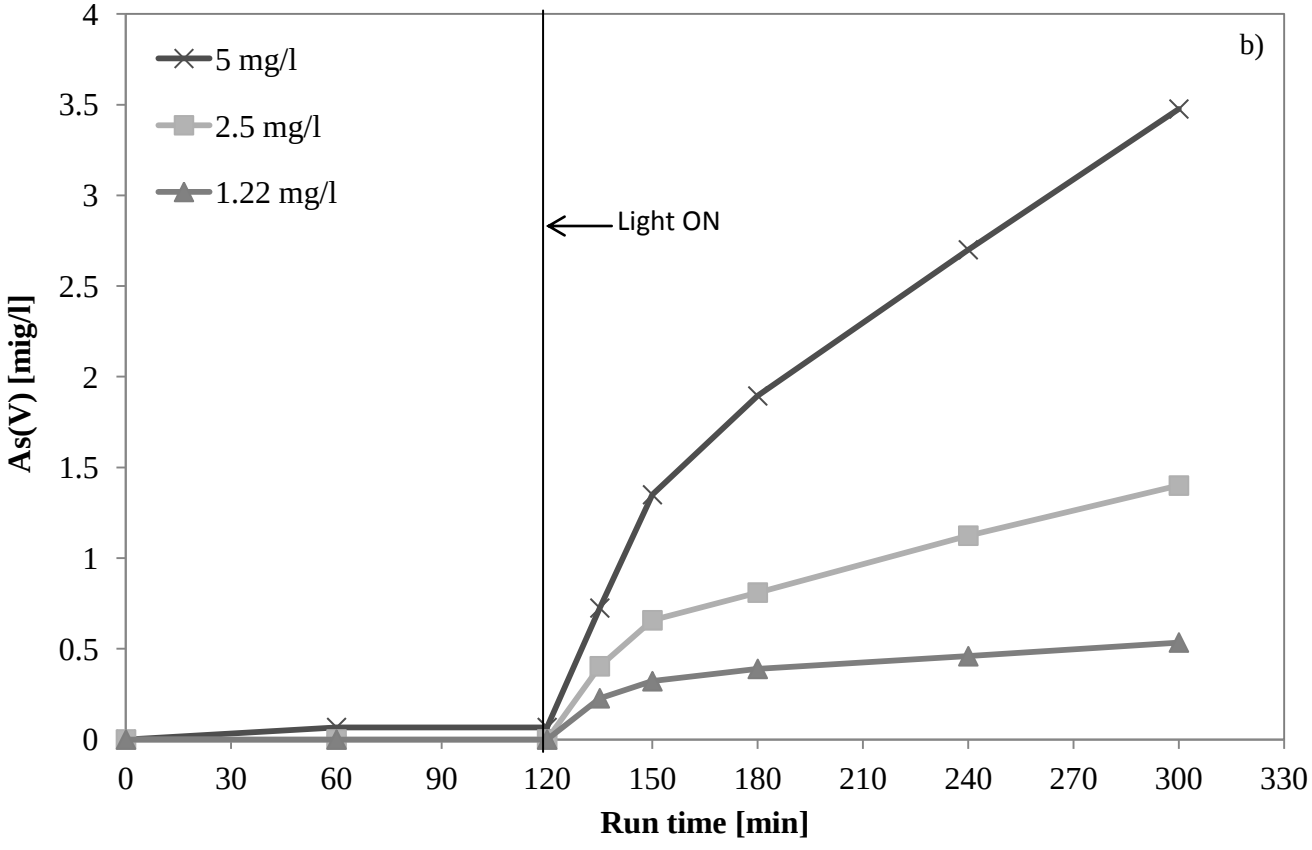

Figure 10: Effect of the initial concentration of As(III) on photocatalytic performances. Behavior of As(III) (a) and As(V) (b); photocatalyst: 1.08 Cu_ZnO; photocatalyst dosage: 3 g/l.

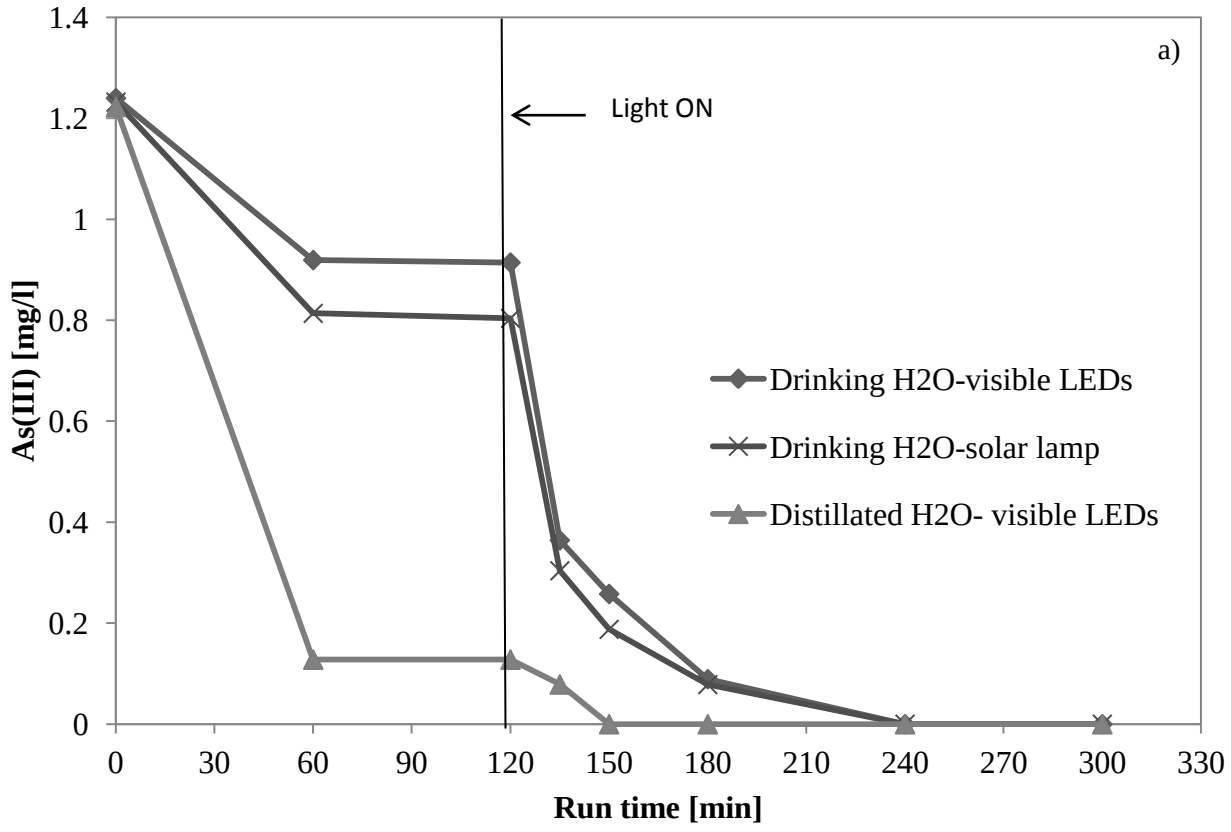

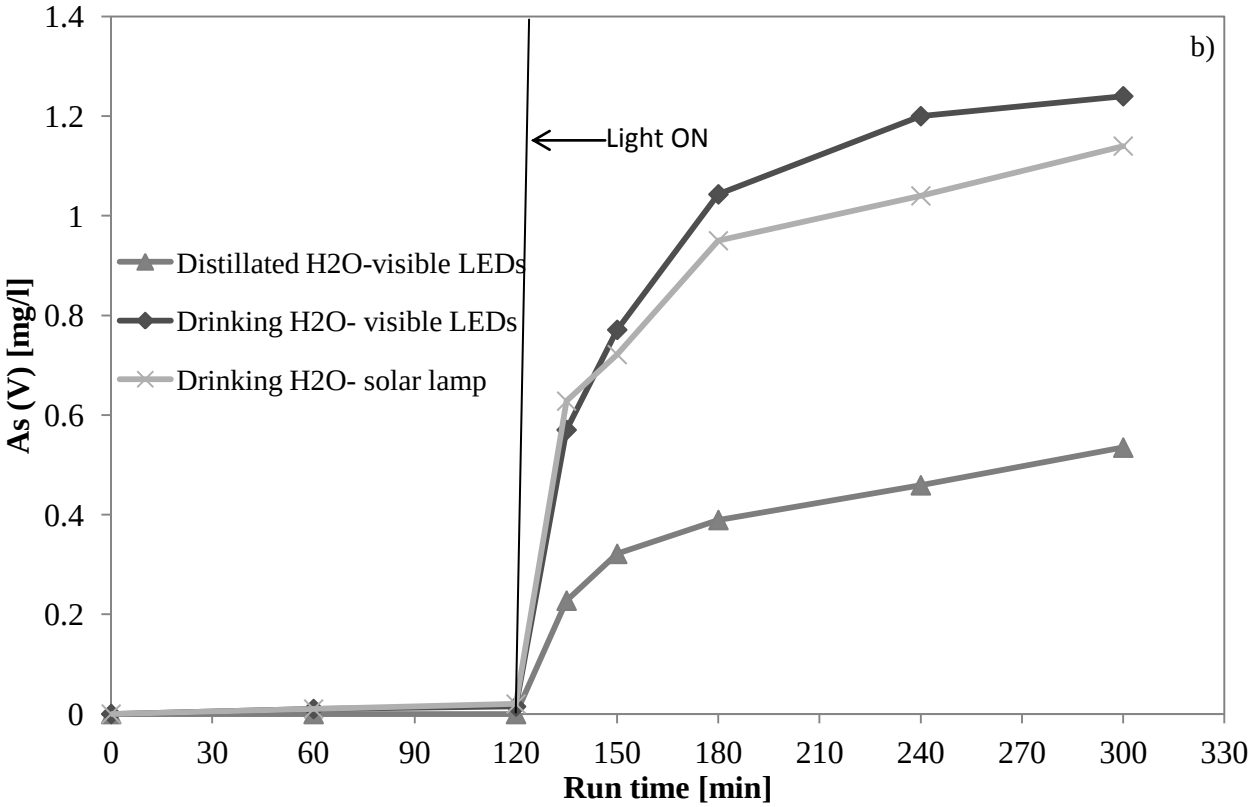

Figure 11: Photocatalytic oxidation of As(III) in distillated and drinking water. Behavior of As(III) (a) and As(V) (b) concentration. Initial As(III) concentration: 1.22 mg/l; photocatalyst: 1.08 Cu_ZnO; photocatalyst dosage: 3 g/l.

***Graphical Abstract**

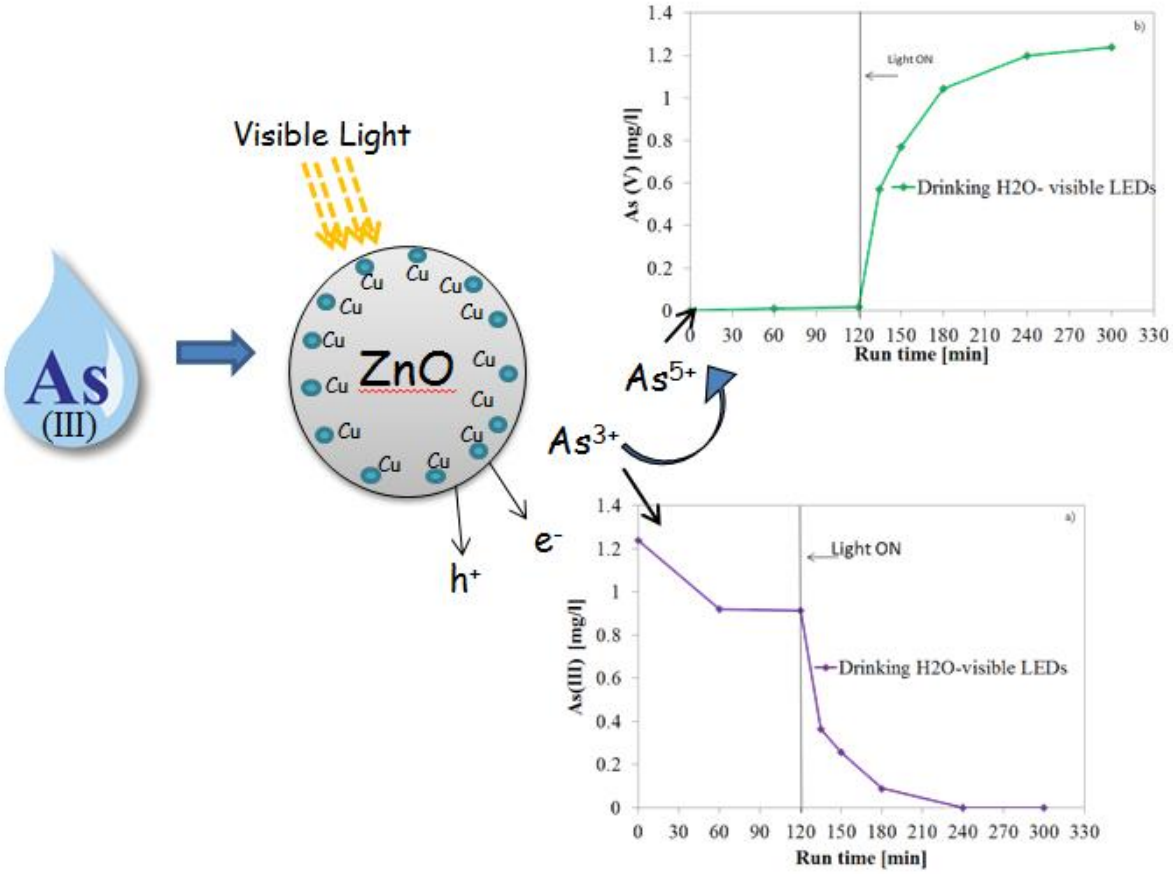

Highlights

- Cu-doped ZnO photocatalysts synthesized through precipitation method.
- Photocatalytic oxidation of As(III) to As(V) under visible light.
- The optimal Cu loading was 1.08 mol%.
- Arsenic removal from drinking water by photocatalytic oxidation.
- Complete As(III) oxidation in presence of solar simulated light.

Supplementary Material

Click here to download Supplementary Material: Supplementary materials.docx